Mechanisms of Ageing and Development 212 (2023) 111820

Contents lists available at ScienceDirect

Mechanisms of Ageing and Development

journal homepage: www.elsevier.com/locate/mechagedev

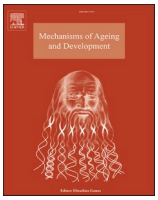

A minimal promoter region of *Kit* gene recapitulates mast cell differentiation in development, aging and inflammation

Serena Fuda [a,1], Daniela F. Angelini [b,1], Ambra Colopi [a,1], Eugenia Guida [a], Angelo Onorato [a], Paola Grimaldi [a], Serena Travaglini [a], Emmanuele A. Jannini [c], Susanna Dolci [a,*]

[a] Department of Biomedicine and Prevention, University of Rome Tor Vergata, Italy
[b] Neuroimmunology Unit, Istituto di Ricovero e Cura a Carattere Scientifico (IRCCS) Santa Lucia Foundation, Rome, Italy
[c] Department of Systems Medicine, University of Rome Tor Vergata, Rome, Italy

ARTICLE INFO

Keywords:
Kit
Mast cell
Gonad
HFD
FceRI

ABSTRACT

To follow mast cells (MCs) distribution during aging and inflammation, we characterized two transgenic mouse models in which the EGFP expression is controlled by 9 kb or 12 kb of *Kit* gene promoter, defined as p18 and p70, respectively. We detected EGFP-positive cells in the serosal surfaces of the peritoneum, pleuras and pericardium, mucosal cavities, and connective tissue of almost all organs including gonads of p70, but not of p18 mice. By FACS and immunofluorescence for FcεR1, Kit and β7-integrin, we found that these EGFP positive cells were MCs. In non-inflammatory conditions, a higher percentage of EGFP positive cells was found in juvenile with respect to adult serosal surfaces, but no differences between males and females at both developmental ages. We found, however, a striking difference in developing gonads, with low numbers of EGFP positive cells in fetal ovaries compared to age matched testes. Under inflammatory conditions caused by high fat diet (HFD), mice showed an increase in serosal EGFP positve cells. Altogether our results identify a regulatory region of the *Kit* gene, activated in MCs and that directing EGFP expression, can be employed to trace this immune cell type throughout the organism and in different animal conditions.

1. Introduction

MCs are immune cells involved in innate and adaptive responses to harmful antigens. They distribute to all vascularized organs and reside within the stroma or the lining epithelia near the external environment. Accordingly, they can be classified into mucosal, if they localize within the epithelial layer or lamina propria of the intestinal and respiratory mucosa, or connective, if they localize within the stromal compartment around venules and nerve endings of most connective tissues. In many animal species, including rodents, connective MCs also reside in serosal cavities, such as peritoneum, pleura, or pericardium. Both cell types originate as MCp from granulocyte/monocyte progenitors (GMPs) in the bone marrow (BM) and migrate at different developmental times throughout the body, to finally differentiate in mature MCs. MCs that colonize mucosal surfaces, such as respiratory or digestive tracts, depend on BM support throughout life, while connective MCs are seeded during late embryonic life to become resident precursors postnatally and expand at necessity (Li et al., 2018). For their survival/proliferation, MCs depend on the expression of the *Kit* gene. It encodes for the transmembrane receptor of the cytokine stem cell factor (SCF or Kit Ligand, KL), that regulates proliferation and/or survival of stem cells from embryonic and postnatal origin. Apart from MCs, *Kit* expression is essential for melanoblasts (MBs), hemopoietic stem cells (HSCs), and PGCs development (Todaro et al., 2019). *Kit* maps at the *W* locus (white spotting) and genomic alterations or loss of function mutations affect the expansion of these stem cell lineages, leading to anemia, sterility and amelanosis. During hemopoiesis and maturation, *Kit* expression is down-regulated in all the descendants of HSCs except for MCp, which is maintained high throughout their maturation (Valent and Bettelheim, 1992). The regulation of *Kit* expression at the transcriptional level in tissue-specific stem cells is mediated by transcription factors (TFs) that belong to the Myc superfamily of bHLH in a tissue specific context. *Tal1* was found to be essential for *Kit* expression in embryonal HSCs, while *Mitf* was identified as the master regulatory TF for *Kit* expression and cell survival in MBs and MCs (Isozaki et al., 1994; Krosl et al., 1998; Yamazaki et al., 1994). Other bHLH TFs were successively identified to

* Corresponding author.
E-mail address: dolci@uniroma2.it (S. Dolci).
[1] Equally contributing authors

https://doi.org/10.1016/j.mad.2023.111820
Received 19 March 2023; Received in revised form 24 April 2023; Accepted 27 April 2023
Available online 11 May 2023

be required for Kit expression in spermatogonia and oocytes (Barrios et al., 2012; Pangas, 2012), while recent studies reported that the pluripotency core TFs *Oct4*, *Nanog* and *Sox2* are critical for *Kit* expression in the inner cell mass (ICM) of the embryo and in embryonic stem cells (ESCs) (Todaro et al., 2019). The regulatory regions that control *Kit* expression in most stem cell types, except for HSCs, are interspersed within 200 kb upstream and 60 kb within the coding sequences of *Kit* gene (Berrozpe et al., 2006), however we identified a minimal promoter region within 6.9 kb from the *Kit* transcriptional start site and 4.5 kb of the first intron, that correctly activates EGFP expression in PGCs and HSCs from *Kit*-promoter EGFP transgenic mice (p18).

Here we show that transgenic mice carrying a larger construct (p70), that includes additional 3 kb of the first *Kit* intron to p18 line, not only show EGFP expression in HSCs and germ cells but also in a cell type that distributes within the stroma of almost every organ and within mucosal and serosal tissues. To validate the identity of these intensely positive EGFP cells, we isolated them from peritoneal, pericardial, or pleural surfaces. We found that these EGFP positive cells showed brighter fluorescence (++) compared to BM cells (+) and resulted positive for Kit (CD117), FcεRI and β7-integrin, cell surface markers that identified both immature and mature MCs. When grown in culture in the presence of SCF and IL-3, these MCs underwent clonal expansion. FACS analysis of serosal EGFP+ + MCs showed a lower percentage in adult animals, that significantly increased following HFD, both in young and adult animals. We also found that connective MCs were more abundant in male gonads at fetal and aging stages compared to female, while in the ovary they were abundant during the reproductive stage. Altogether our results show that (1) 12 kb of the *Kit* promoter region are sufficient to promote mast cell specific EGFP expression; (2) both immature and mature MC show EGFP expression in mucosal as well as connective localizations, (3) gonadal mast cells show a dimorphic distribution. Altogether our results show that *Kit*-promoter EGFP+ + MC are a new tool to dynamically trace mast cell migration and maturation in physiological and pathological conditions.

2. Materials and methods

2.1. Mice

Generation of p18 and p70 transgenic mice have been previously described (Cairns et al., 2003), and outlined in Fig. 1. To obtain experimental animals, we crossed C57Bl/6 with CD1 albino mice. F1 generation was used throughout the experiments. For genotyping, DNA extracted from tails was PCR amplified by using primers obtained on EGFP ORF (EGFP 5'-GCATACCCATACGATGTTCC forward and EGFP 5'-TGAAGTTCACCTTGATGCCG reverse primers). Embryos were collected at day 15 after vaginal plug (days post coitum, dpc).

2.2. High fat diet

Ten 2 months old experimental animals (see above) were divided into two groups: the control group (Ctr) was supplied with a normal diet for 12 weeks, while the high-fat diet group (HFD) was supplied with a 60 kcal% fat diet (D12492, Research Diets, New Brunswick, New Jersey, US) for 12 weeks. At the end of the treatment adult mice were sacrificed. The weight of mice was monitored once a month. Both control and HFD-treated offspring were subjected to flow cytometric analysis at 8 dpp.

2.3. Isolation of mast cells

To isolate mast cells from the peritoneal cavity an incision was made in the abdominal skin of sacrificed mice. Using a 1 mL syringe, PBS (ECB4004L, EuroClone, Milano, Italy) was injected into the peritoneal cavity to collect the cell-containing fluid.

BM cells were collected by harvesting the femur from the hip joint to the knee joint. Using a 1 mL syringe, PBS was flushed through the BM and the fluid was collected. Red blood cell (RBC) lysis buffer (00–4333–57, Thermo Fisher Scientific, Waltham, Massachusetts, US) was performed on the collected fluid to eliminate RBC.

To obtain pleural and pericardial mast cells, heart and lungs were incubated with 0,5 mg/mL collagenase (11088858001, Merk) solution at 37 °C for 15 min and cells were then collected.

2.4. Histology

Histological analyses were performed on fresh 5 μm tissue sections embedded in OCT (361603E, VWR, Radnor, USA). Nuclei were stained with Hoechst (62249, Thermo Fisher Scientific).

Isolated cells from the peritoneal cavity were centrifuged at 1400 rpm for 5 min and resuspended in PBS. A drop of the cell suspension was spread on a slide to form a thin layer and air-dried. Cells were stained with a toluidine blue solution prepared by dissolving 0,025 g of toluidine blue in 30 mL of absolute ethanol and 400μL of glacial acetic acid, adding distilled water to make a total volume of 100 mL. For gonadal counts, EGFP++ cells were counted from 10 consecutive sections of 15 μm thickness from 3 independent gonads. Since oocytes and differentiating spermatogonia are the major source of Kit expressing cells and thus are potential EGFP expressing cells, in the postnatal gonads we considered EGFP++ MCs only those cells that did not show germ cell features, to prevent errors in MC detection. In the ovaries, EGFP+ growing oocytes were easily identified by their abundant cytoplasm while those included in primordial follicles localized in the cortical region of the organ. Thus, only positive cells that were localized outside the follicles, within the medullary region and with obvious scant cytoplasm, were assessed. In the testis, EGFP++ cells were found within the interstitial tissue delimited by the seminiferous tubules, while differentiating spermatogonia localize in the basal layer of the seminiferous tubules. Numbers are represented per microscopic field at 200X magnification.

2.5. Immunofluorescence

Cells were fixed in 4 % PFA (AR1068, Boster Biological Technology, Pleasanton, California, US), permeabilized with 0.1 % Triton (X100–500 mL, Merk) solution in PBS and blocked in 0.5 % BSA. Cells were incubated with anti-Kit (#3074, Cell Signaling Technology, 1:100) and anti-FcεR1 (sc-390222, Santa Cruz Biotechnology, Dallas, Texas, US, 1:100) primary antibodies. Anti-mouse Alexa Fluor® 594-conjugated (115–585–166, Jackson Immunoresearch Europe Ltd, Cambridge House, St. Thomas Place, UK, 1:200) was used as secondary antibody. Nuclei were stained with Hoechst (62249, Thermo Fisher Scientific, 1:10000).

2.6. Flow cytometry

Cells isolated from peritoneum, BM, heart and lungs were labeled with a dead cell labeling probe, LIVE/DEAD Fixable Aqua Dead Cell Stain Kit (L34957, Thermo Fischer Scientific) and the following anti-mouse antibodies conjugated to the appropriate fluorochrome: CD45 conjugated to PercP5.5 (1115660, SONY); Kit (5553355, BD Pharmingen, Budapest, Hungary) and β7-integrin (557498, BD Pharmingen) conjugated in PE; FcεR1 conjugated in APC (17–5898–82, e-Bioscience). Stained cells were acquired on a CytoFLEX flow cytometer (Beckman Coulter), equipped with five lasers and able to measure up to 23 parameters simultaneously on each cell. For each sample, approximately 300,000 cells were selected based on scatter parameters, and the analysis was conducted after the exclusion of dead cells and coincident events. Data were compensated and analyzed using FlowJo v10.8.1 (Becton Dickinson & Company).

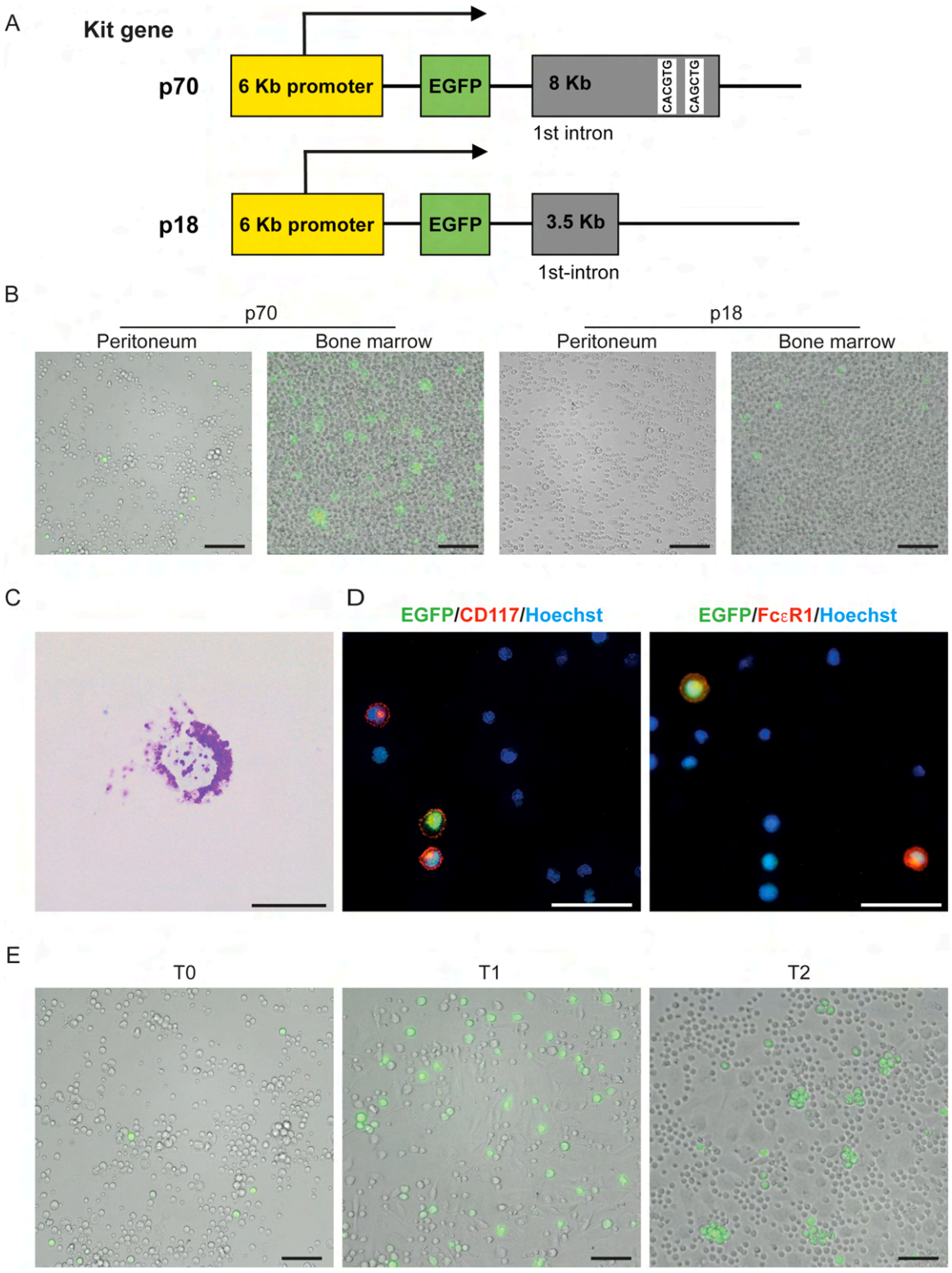

Fig. 1. EGFP is expressed in p70 peritoneal and BM MCs. (A) Schematic representation of p70 and p18 transgenes. (B) Light microscopy images of EGFP expression in peritoneal and BM compartments of p70 and p18 mice. Scale bar = 50 μm. N = 6. (C) Light microscopy image of a p70 peritoneal cell stained with Toluidine blue. Scale bar = 25 μm. N = 3. (D) Immunofluorescence analysis on p70 peritoneal EGFP+ + cells for cell surface marker CD117 (left panel) and high-affinity IgE receptor FcεR1 (right panel). Scale bar = 50 μm. N = 4. (E) Light microscopy images of p70 peritoneal cells in culture for 0 h (T0, left panel), 24 h (T1, middle panel) and 72 h (T2, right panel). Scale bar = 50 μm. N = 3.

2.7. Cell cultures

MCs collected from peritoneal fluid were purified using α-CD117 microbeads (120–001–554, Miltenyi Biotec, Bergisch Gladbach, Germany) and separated into two populations: the first one was cultured in StemSpan™ SFEM II (09605, StemCell Technologies, Vancouver, Canada) supplemented with StemSpan™ CD34 + Expansion Supplement (02691, StemCell Technologies); the second population was cultured in DMEM (21969035, Thermo Fisher Scientific) supplemented with 10 ng/mL SCF (250–03, PeproTech, London, UK) and 10 ng/mL IL-3 (213–13, PeproTech).

Cells were grown in a 37 °C humidified atmosphere of 5% CO_2.

2.8. Statistical analysis

All analyses were performed with Prism 7 software. Results are shown as mean±SEM (standard error of mean). Statistical tests were considered significant for relative values $p < 0.05$. All experiments were performed on at least three biological replicates.

3. Results

3.1. 12 kb kit promoter induces EGFP expression in MCs

We have previously shown that p18 and p70 mouse models specifically express EGFP in PGCs and BM stem cells compartments under the control of *Kit* regulatory regions (Cairns et al., 2003). We observed that other cells in adult p70 but not in p18 mice, showed bright EGFP fluorescence when isolated from the surface of peritoneal organs. In particular, we found that following peritoneal lavage, a consistent amount of small-intermediate (15–20 μm diameter) EGFP++ cells were recovered. These intensely fluorescent cells were not identified in the same compartments of p18 mice (Fig. 1B). Purification of peritoneal fluid by immunomagnetic sorting with CD117 magnetic beads followed by smearing and staining with Toluidine Blue suggested that they were MCs (Fig. 1C). By immunofluorescence analysis we found that the EGFP++ cells within the peritoneal fluid stained positive for FcεR1, that marks MCs and basophils, and CD117, that is specific for MCs (Fig. 1D). By culturing them in DMEM medium supplemented with 50 ng/mL SCF or in StemSpan SFEM II with CD34 + supplement to allow their expansion, we found a strong increase of EGFP+ + cells and colonies formation in both conditions after 3 days *in vitro* (Fig. 1E).

3.2. Serosal EGFP++ MCs are more abundant in prepuberal compared to aging mice

It has been reported that connective MCs increase with age (Kutukova et al., 2016) although C57Bl/6 and Balb/C mice show a reduction of dermal MCs during late stages of life (Hart et al., 1999). To assess a potential age-related decrease in serosal MCs, we evaluated EGFP++ cells distribution in p70 mice peritoneal surface, pericardium, and pleura. To this end we isolated hearts and lungs from adult (4–6 months old, mo) or prepuberal mice (8 days post-partum, dpp) that were observed in whole mount preparations. As shown in Fig. 2A, we found few scattered cells brightly fluorescent and elongated on the surface of adult hearts and lungs. Frozen sections obtained from fixed organs confirmed the presence of clusters of EGFP++ cells on the surface of the heart and within the myocardium. Adult lungs showed scant EGFP++ cells on the visceral pleura and within the alveolar septi. When observing organs from prepuberal mice, we found that heart surface was completely covered by bright EGFP++ cells, and the same result was confirmed in frozen sections (Fig. 2B). In addition, higher number/-surface of EGFP++ cells were found within the myocardium, predominantly in the atrial compartments. Although less abundant than onto heart surfaces, EGFP++ cells were found also on prepuberal lung surfaces and within the alveolar septi. Both heart and lung recovered EGFP++ cells were more prominent in young compared to adult organs (Fig. 2B). To follow serosal colonization during development, we inspected frozen sections obtained from p70 embryos at 15.5 dpc, a developmental stage when FCεRI$^-$ MCps are found differentiating from yolk sac haemopoietic stem cells (Gentek et al., 2018). Interestingly, we found that many EGFP++ cells were already present in the peritoneal cavity, onto ventricular epicardium and within the atrial myocardium as well as in liver and skin, but not in the fetal lungs (Fig. 2C). To confirm that the also the EGFP++ cells located onto the epicardium or pleura were bona-fide MCs, we isolated them from adult and prepuberal mice by mild collagenase treatment of whole hearts and lungs and subjected them to flow cytometry along with peritoneal cells. To identify MCs, we utilized antibodies against FcεR1 and β7-integrin, the latter specific for MCp and MCs, and CD117. We first set gating on CD45 + cells to preselect immune cells from each compartment containing EGFP++ cells. Then we analyzed the population of peritoneal, pericardial, and pleural MCs according to the expression of EGFP, CD117 and FcεR1 markers, to identify the cell population with the highest expression levels of the three markers. In a separate setting we detected EGFP and β7-integrin within the CD45+ population. We found that the percentage of EGFP++ CD117 + recovered cells was about 1.29% in adult peritoneum, 0.088 % in the pericardium and almost undetectable (0 %) in the pleura (Fig. 3 A). On the contrary, we observed a higher percentage of double positive cells in all the preparations from prepuberal serosae (1.98 % in the peritoneum, 1.23 % in the pericardium and 0.30% in the pleura) (Fig. 3A). Interestingly, we noticed that the median EGFP fluorescence intensity was significantly higher in prepuberal peritoneal MCs when compared to their adult counterparts (2-fold increase), while median CD117 fluorescence intensity did not significantly change (Fig. 3B). All the EGFP++ cells in the peritoneum showed a median FcεR1 and β7-integrin fluorescence intensity similar at both developmental ages, indicating they were mature MCs (Supplemental Fig. 2A).

3.3. Peritoneal EGFP++ MCs are increased in HFD-treated mice

It has been reported that *ob/ob* mice show increased numbers of MCs in abdominal fat depots (Altintas et al., 2012). To understand if our model could recapitulate the obesity induced inflammatory condition, we subjected p70 mice to HFD. Body weight increasing have been observed and the reproductive rate have been monitoring during the treatment (Supplemental Fig. 1A-B). We evaluated EGFP++ cells abundance in both p70 HFD-treated and conventionally fed mice. Analyses were performed on MCs obtained from BM and from peritoneal cell suspension of both adult and prepuberal mice. HFD-treated mouse pups were obtained from HFD mothers maintained on obesogenic diet during the lactation period. As shown in Fig. 4A-C, we found that the number of EGFP++ CD117+ MCs increased in the peritoneal fluid of HFD-treated mice from about 1.29 % to 3,09 % when compared to conventionally fed mice. The median EGFP, FcεR1 or β7-integrin fluorescence intensity, instead, did not significantly differ between the two conditions both in the peritoneal fluid and in BM (Fig. 4C and Supplemental Fig. 2B). When we observed the peritoneal fluid from control and HFD-treated prepuberal mice, we found a similar behavior of EGFP++ CD117+ MCs as for the adult condition. The percentage of positive cells, in fact, increased from 1.90 % to 3.34 % (Fig. 4B-C). Moreover, the median EGFP fluorescence intensity was significantly higher in HFD treated pups (Fig. 4C), showing a 2-fold increase with respect to control fed pups. On the contrary, the levels of FcεR1 and β7-integrin did not change (Suppl.2B). BM-derived cells showed a statistically significant difference in EGFP++ CD117+ MCs percentage between young and adult animals (Fig. 3C). On the other side, no differences in EGFP++ CD117+ BM-derived MCs percentage, nor in the median EGFP, FcεR1 and β7-integrin fluorescence intensity were found between HFD- and regular diet-treated mice (Supplemental Fig. 2B-C).

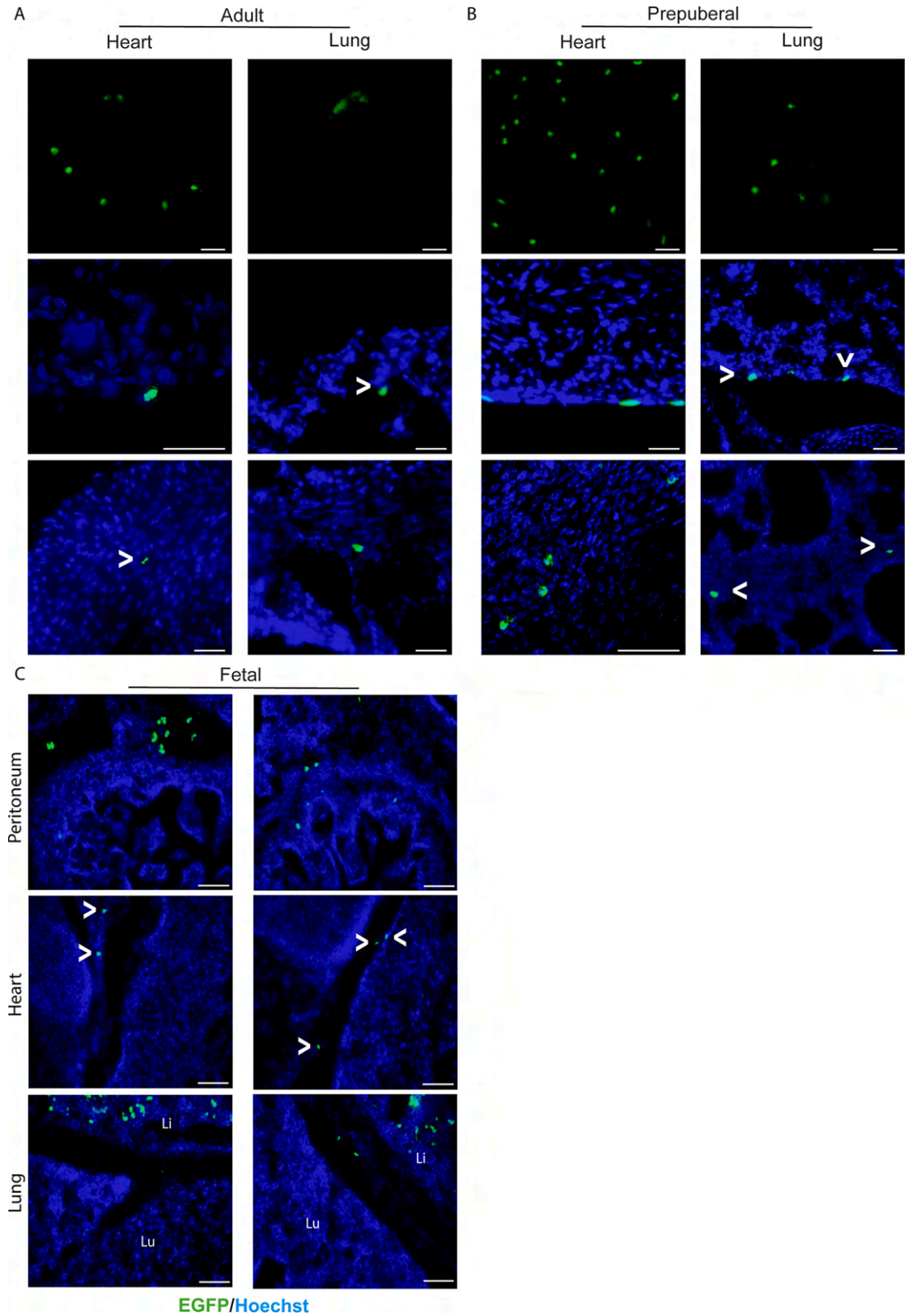

Fig. 2. EGFP++ MC localize onto serosal surfaces of heart and lungs and within the myocardium and the alveolar septi. (A) Whole mount preparations (upper row) and frozen sections (middle and lower row) of adult p70 heart or lungs showing EGFP-expressing MCs onto epicardium and visceral pleuras and within heart and lung parenchyma. Scale bar = 25 μm. (B) Whole mount preparations (upper row) and frozen sections (middle and lower row) of prepuberal p70 heart or lungs showing EGFP-expressing MCs onto epicardium and visceral pleuras and within heart and lung parenchyma. Scale bar = 25 μm. (C) Histological analysis of EGFP-expressing cells on frozen sections of peritoneal cavity, heart and lungs from p70 embryos. Lu = lung, Li = liver, G=gut. Scale bar = 75 μm. Arrows indicate EGFP++ cells. N = 3.

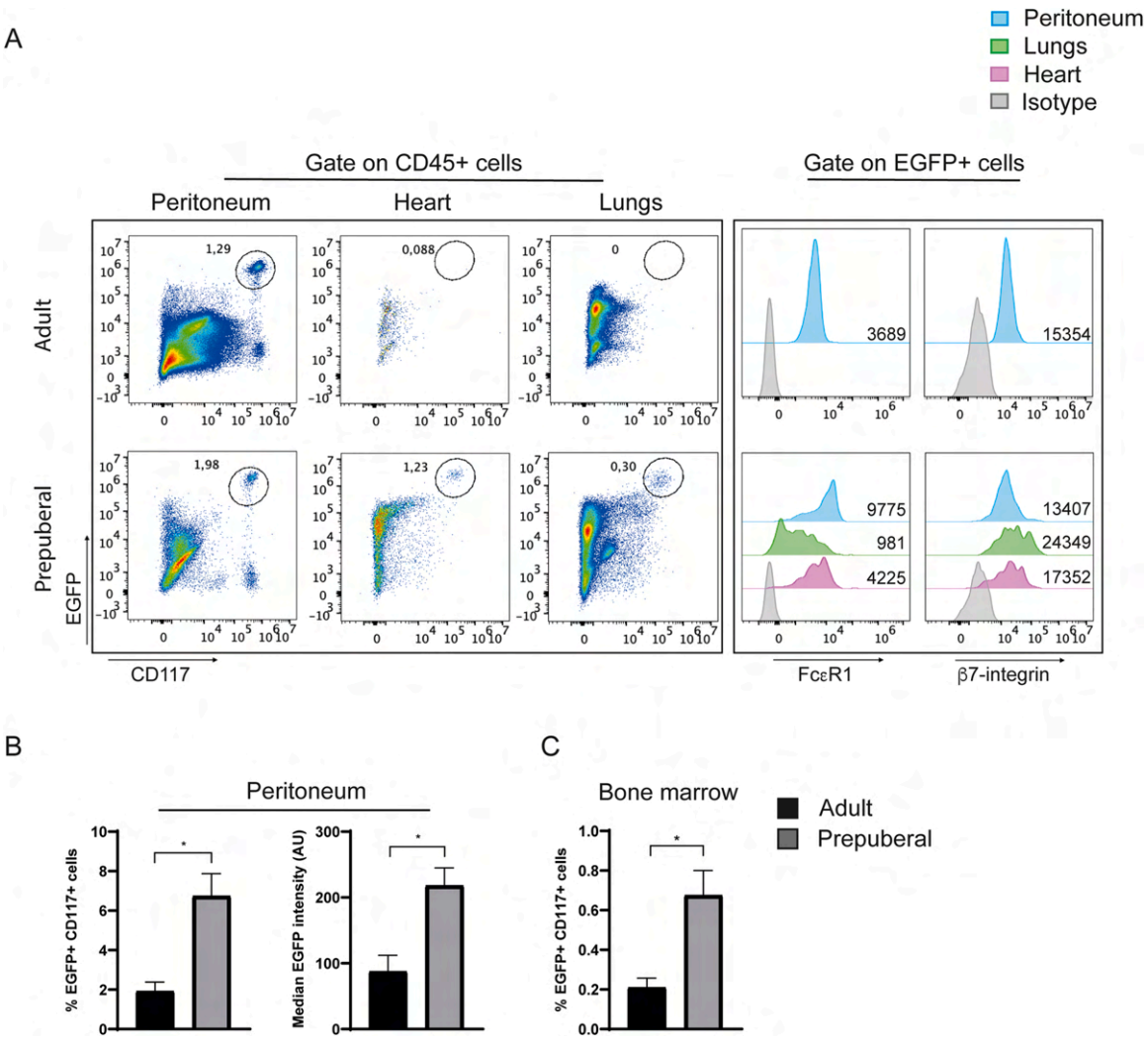

Fig. 3. EGFP++ MCs are more abundant in prepuberal serosal compartments compared to adult p70 mice. (A) Flow cytometric analysis of EGFP++ CD117 + cells isolated from peritoneum, heart, and lungs of adult (upper row) and prepuberal (lower row) p70 mice. Left panel shows the percentage of EGFP++ CD117+ cells gated on total CD45+ cells. Right panel shows FcεR1, and β7-integrin expression levels gated on EGFP++ cells from peritoneum (light blue), heart (pink) and lungs (green). FcεR1 and β7-integrin expression level was determined as median of fluorescence (reported on histograms). In gray the isotype control. N = 3. (B) Comparative analysis between adult and prepuberal peritoneal fluid showing EGFP+ + CD117 + cells distribution and median EGFP fluorescence intensity of EGFP++ CD117+ cells. N = 3. (C) Comparative analysis between adult and prepuberal BM-derived EGFP++ CD117+ cells distribution. N = 3. AU = Arbitrary Units. Mean±SEM * $p < 0.05$, unpaired t test.

3.4. *EGFP++ MCs show dimorphic distribution in fetal and adult gonads*

We did not detect any sex differences in EGFP++ MCs distribution during fetal and postnatal development between male and female age matched organs (not shown), except for gonads.

When analyzing fetal organs, we found a striking difference in MC gonadal colonization between ovary and testis at 15.5 dpc, a stage at which Kit and EGFP are barely detected in germ cells. We counted EGFP++ cells in frozen sections, and found that, while the fetal ovary was almost completely devoid of MCs (2 ±1/microscopic field), the fetal testis contained many EGFP++ cells scattered throughout the interstitial spaces within adjacent tubules (30 ±8/microscopic field) (Fig. 5A).

Such difference was reduced between the two sexes in young adult gonads, when ovarian EGFP++ MCs were found scattered around growing follicles and within the medullary region, and their numbers were strongly increased (about 23 +10/microscopic field). Age matched testicular MCs were localized within the interstitial spaces and their numbers per area were similar (20 +2/microscopic field) as for the ovary (Fig. 5B). Aging ovaries on the contrary, showed very low numbers of MCs (3 +2/microscopic field) localizing only within the hilum of the organ, while aging testes contained similar MC numbers compared to young adult testes (Fig. 5C). While we easily identified EGFP++ MCs in postnatal testes, we found that spermatogonia were EGFP negative, differently from what we previously reported in p18 transgenic animals (Pellegrini et al., 2008), as well as Leydig cells, that also express Kit in the postnatal development (not shown).

4. Discussion

We previously demonstrated that regulatory regions present within 6.9 kb upstream the transcriptional start site of *Kit* gene and the initial 8 kb of the first intron can direct EGFP expression in HSCs of p70 transgenic mouse model (Cairns et al., 2003). The construct utilized for p70 transgenic mice engineering contains multiple highly sensitive DNaseI sites (HS1–6) that localize within the promoter and the first intron. These sites conferred strong tissue specificity and increased expression levels of EGFP in BM. p18 transgenic line, instead, carries a shorter fragment of the first intron, and HSCs express low levels of EGFP in BM. In the present work, we identify an additional cell type originating from BM, the MC, selectively expressing EGFP at higher levels

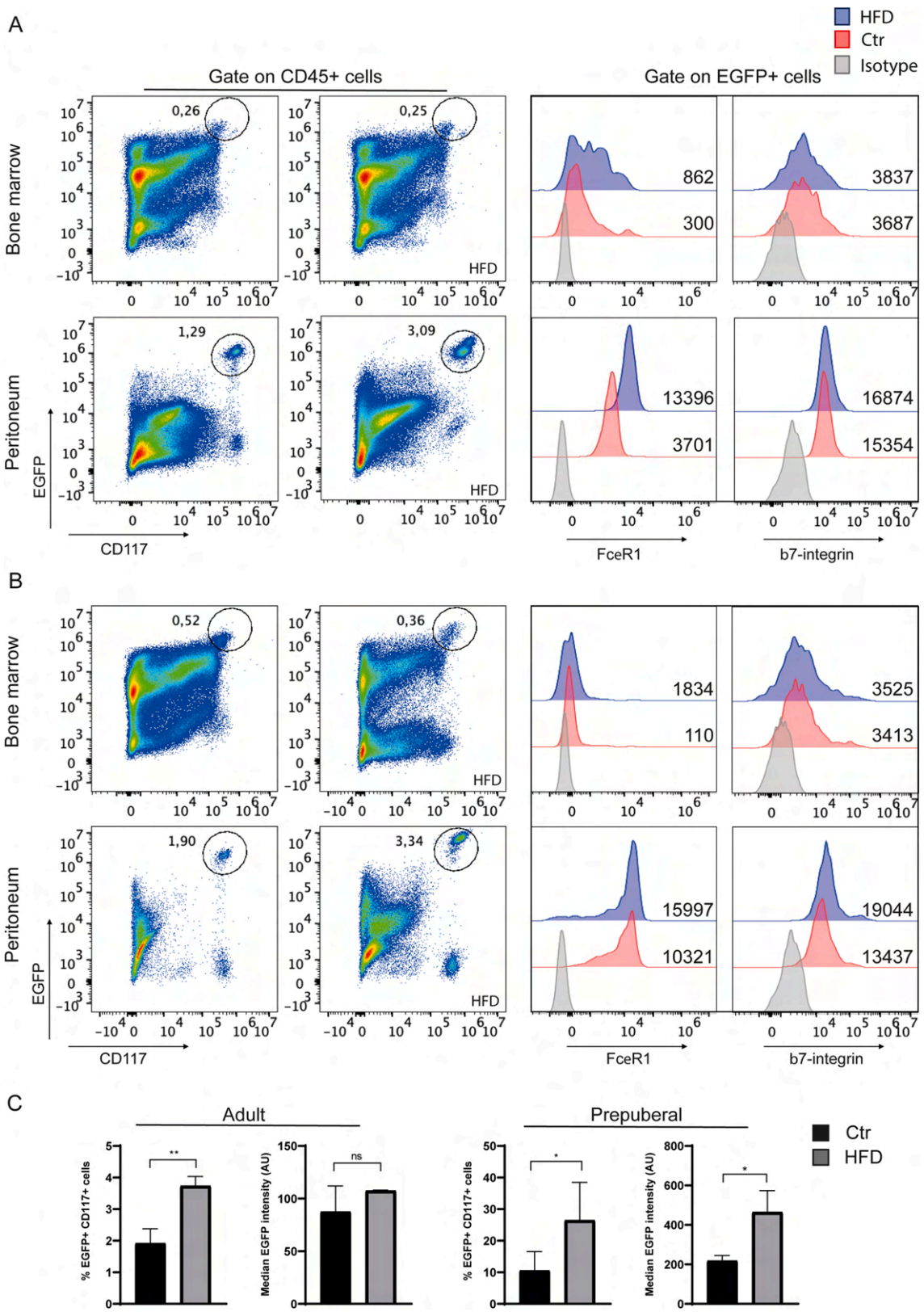

Fig. 4. EGFP++ MCs are increased in p70 HFD-treated mice peritoneum. (A-B) Flow cytometric analysis of EGFP++ CD117+ cells isolated from peritoneum and BM of conventionally fed and HFD-treated p70 adult (A) and prepuberal (B) mice. Left panels (both in A and B) show the percentage of EGFP++ CD117+ cells gated on total CD45+ cells. Right panels (both in A and B) show FcεR1 and β7-integrin expression levels in EGFP++ cells of conventionally fed mice (red) and HFD-treated mice (blue). FcεR1 and β7-integrin expression level was determined as median of fluorescence (reported on histograms). In gray the isotype control. N = 3. (C) Comparative analysis of peritoneal fluid showing EGFP++ CD117+ cell distribution, and median EGFP fluorescence intensity of EGFP++ CD117+ between conventionally fed and HFD-treated adult and prepuberal mice. N = 3 AU = Arbitrary Units. Mean±SEM *$p < 0.05$, * * $p < 0.01$, unpaired t test.

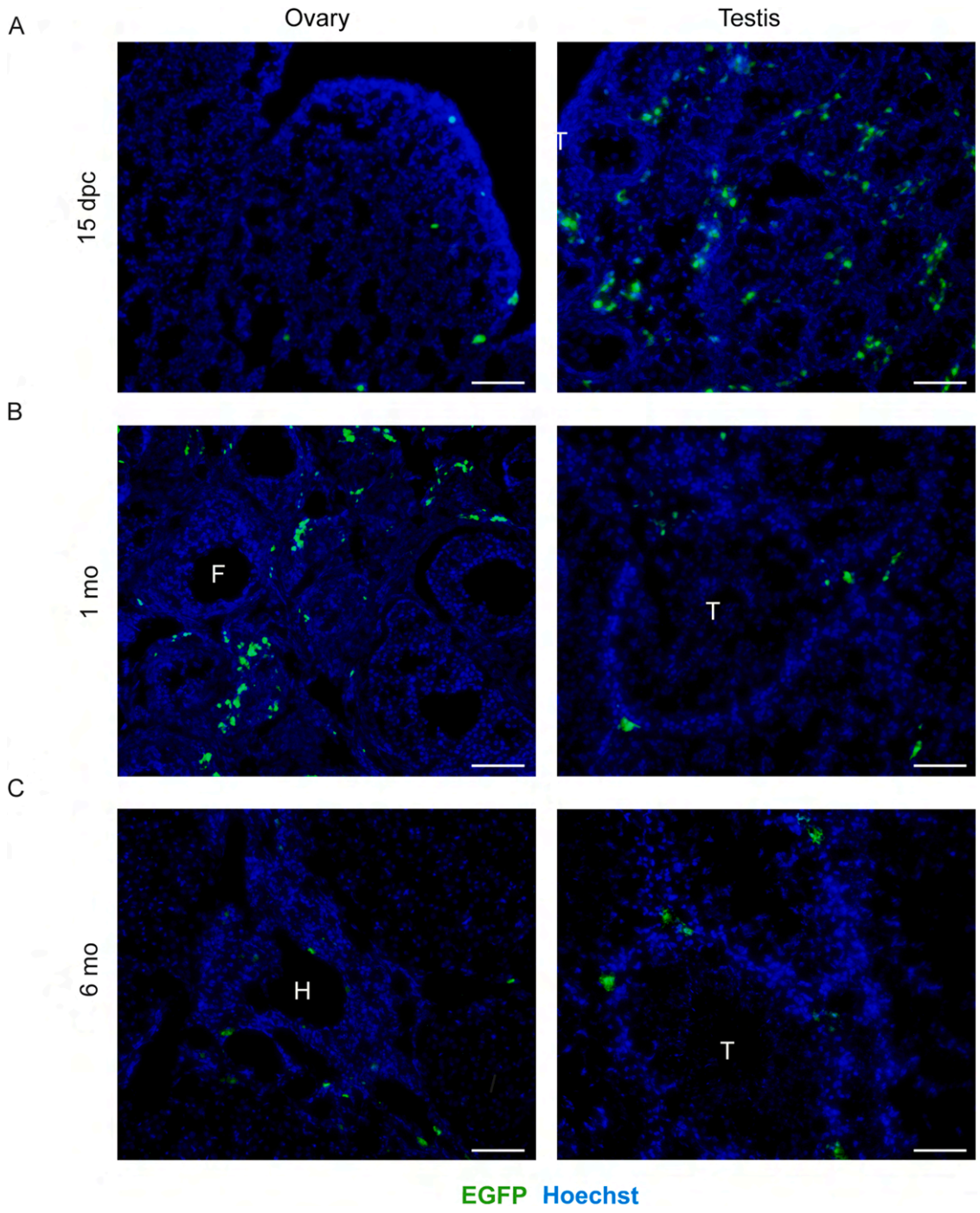

Fig. 5. Male and female gonads are differently colonized by EGFP++ MCs. A-C) Histological analysis of EGFP-expressing cells on representative frozen sections of ovaries (panels on the left) and testes (panels on the right) from 15 dpc, (A) 1 month (mo) (B) and 6 mo. (C) p70 mice. Scale bar = 75 μm. N = 3 samples/developmental age.

compared to HSCs, only in p70 mice. By searching for consensus sequences compatible for bHLH binding sites (CANNTG), within the exclusive 4.5 kb of p70 construct, we identified two p70 specific sequences (Fig. 1 A) that can be potentially recognized by MITF, the specific TF necessary for MC and melanocyte lineages and that are not included in the p18 construct. Characterization of the EGFP++ population by FACS analysis showed that these cells are indeed MCs, as they are CD117+, FcεR1+ and β7-integrin+. Also, they segregate from the remaining BM cell population, since they show brighter EGFP and CD117 fluorescence intensities (++, high) compared to the BM HSCs.

EGFP++ CD117+ FcεRI+ cells are found in association with serosal surfaces as well as with the parenchyma of heart and lung. We found that these sites are differentially repopulated during aging, and prepuberal mice show a higher percentage of EGFP+ + CD117+ FcεRI+ cells on total CD45+ cells in the peritoneal fluid or localized onto epicardial and visceral pleural surface compared to adult animals. EGFP fluorescence intensity of young MCs was higher compared to adult cells, indicating a higher promoter/enhancer activity. However, Kit expression levels did not differ significantly between the two groups, suggesting that other regulatory regions within *Kit* locus participate in the regulation of its expression. Indeed, within 200 kb 5' upstream to the transcriptional DNaseI HSs site have been demonstrated to be critical for locus control

region-mediated *Kit* gene activation in MCs (Berrozpe et al., 2006).

Although it has been shown that MCs numbers increase with age in the dermis, in the gut and in the brain (Blasco et al., 2020; Kutukova et al., 2016), we found that EGFP++ MC numbers were lower in the serosal compartments from adult mice compared to young animals. EGFP++ MCs were detected at as early as 15.5 dpc of development onto the fetal serosal surfaces of peritoneum and epicardium but not of pleuras and their numbers increased in prepuberal mice. Moreover, in inflammatory conditions, such as those induced by HFD, we observed an expansion in peritoneal MC population compared to the regular diet condition, both in adult and young animals. This result is in agreement with the observation that MC increase in adipose tissue of obese mice and humans and contribute to diet-induced obesity and diabetes (Liu et al., 2009). Moreover, our data add an important concept that also at young age HFD is a potent stimulus for MC expansion in the peritoneal fluid. As for normal conditions, MC numbers were significantly higher in young compared to adult animals also in HFD. Similarly, also BM-derived MC numbers were higher in young animals with respect to adults, however they did not significantly differ between HFD and regular diet. MCp in the BM represent a continuous post-natal source of mucosal MCs, while connective MCs derive from BM-MCp during the last embryonic period (Li et al., 2018). Since serosal MCs belong to the connective type differentiating from resident MCp and do not directly originate from BM, our results suggest that in normal conditions aging serosal MCs proliferate slower when compared to their young counterparts.

MC-associated disorders exhibit sex biases, with females at increased risk (Loewendorf et al., 2016; Webb and Lieberman, 2006). At the basis of MC sexual dimorphism is the observation that MCs express sex hormone receptors and respond to the hormonal environment in which they reside. Accordingly, female MCs respond to sexual hormones by storing mediators such as histamine and proteases within their secretory granules with higher capacity and by increasing their degranulation activity (Mackey et al., 2016; Zierau et al., 2012). Moreover, ovarian and uterine MC numbers increase during the estrous cycle in the rat demonstrating a role of gonadal hormones in their recruitment to the reproductive organs (Aydin et al., 1998). While we did not find any significant differences in the peritoneum, heart, or lungs between the two sexes, we found that MCs differently populated male and female gonads. While MCs colonized fetal testes in large numbers compared to age matched ovaries, abundant MC perifollicular colonization was found only in young adult animals, in the active ovary, to decline sharply in the aging organ when follicle numbers decrease, suggesting that they might play a role in MC homing and expansion. On the contrary, male MCs were scattered in the tubular interstitium early during fetal development and their localization and density did not change with aging.

Another important observation we obtained from our study is that Kit promoter activity is differentially regulated in the two sexes, as EGFP expression was present in postnatal oocytes but not in differentiating spermatogonia. Since both spermatogonia and oocytes express high EGFP levels in p18 transgenic animals (Filipponi et al., 2007; Rossi et al., 2017), a repressive role of the genomic regions contained within the 4.5 kb fragment exclusive to the p70 construct can be hypothesized. These results unveil a sexual dimorphism in MCs distribution during gonad developmental and a sexually dimorphic regulation of Kit promoter activity in male and female germ cells.

In summary, we identified an additional regulatory region of the *Kit* gene located within its first intron, that acts as a specific enhancer for fetal and postnatal MCs. p70 mice represent a useful model to study MC distribution in adult and young animals of both sexes and to trace them in healthy or pathological conditions. Moreover, the possibility to isolate and culture MCs as pure cell populations by sorting them for EGFP fluorescence, makes our animal model a new tool to study MC biology.

Data availability

Data will be made available on request.

Acknowledgments

We thank Mr Fabio Lancia and Mrs Maura Paglialunga for animal husbandry. This work was supported by grants from the Ministero dell'Università e della Ricerca. [grant number 2020XMLP45_004 and 2017S9KTNE_002].

Appendix A. Supporting information

Supplementary data associated with this article can be found in the online version at doi:10.1016/j.mad.2023.111820.

References

Altintas, M.M., Nayer, B., Walford, E.C., Johnson, K.B., Gaidosh, G., Reiser, J., De La Cruz-Munoz, N., Ortega, L.M., Nayer, A., 2012. Leptin deficiency-induced obesity affects the density of mast cells in abdominal fat depots and lymph nodes in mice. Lipids Health Dis. 11, 21.

Aydin, Y., Tuncel, N., Gurer, F., Tuncel, M., Kosar, M., Oflaz, G., 1998. Ovarian, uterine and brain mast cells in female rats: cyclic changes and contribution to tissue histamine. Comp. Biochem. Physiol. A Mol. Integr. Physiol. 120, 255–262.

Barrios, F., Filipponi, D., Campolo, F., Gori, M., Bramucci, F., Pellegrini, M., Ottolenghi, S., Rossi, P., Jannini, E.A., Dolci, S., 2012. SOHLH1 and SOHLH2 control kit expression during postnatal male germ cell development. J. Cell Sci. 125, 1455–1464.

Berrozpe, G., Agosti, V., Tucker, C., Blanpain, C., Manova, K., Besmer, P., 2006. A distant upstream locus control region is critical for expression of the Kit receptor gene in mast cells. Mol. Cell Biol. 26, 5850–5860.

Blasco, M.P., Chauhan, A., Honarpisheh, P., Ahnstedt, H., d'Aigle, J., Ganesan, A., Ayyaswamy, S., Blixt, F., Venable, S., Major, A., Durgan, D., Haag, A., Kofler, J., Bryan, R., McCullough, L.D., Ganesh, B.P., 2020. Age-dependent involvement of gut mast cells and histamine in post-stroke inflammation. J. Neuroinflamm. 17, 160.

Cairns, L.A., Moroni, E., Levantini, E., Giorgetti, A., Klinger, F.G., Ronzoni, S., Tatangelo, L., Tiveron, C., De Felici, M., Dolci, S., Magli, M.C., Giglioni, B., Ottolenghi, S., 2003. Kit regulatory elements required for expression in developing hematopoietic and germ cell lineages. Blood 102, 3954–3962.

Filipponi, D., Hobbs, R.M., Ottolenghi, S., Rossi, P., Jannini, E.A., Pandolfi, P.P., Dolci, S., 2007. Repression of kit expression by Plzf in germ cells. Mol. Cell Biol. 27, 6770–6781.

Gentek, R., Ghigo, C., Hoeffel, G., Bulle, M.J., Msallam, R., Gautier, G., Launay, P., Chen, J., Ginhoux, F., Bajenoff, M., 2018. Hemogenic endothelial fate mapping reveals dual developmental origin of mast cells. Immunity 48 (1160–1171), e1165.

Hart, P.H., Grimbaldeston, M.A., Hosszu, E.K., Swift, G.J., Noonan, F.P., Finlay-Jones, J. J., 1999. Age-related changes in dermal mast cell prevalence in BALB/c mice: functional importance and correlation with dermal mast cell expression of Kit. Immunology 98, 352–356.

Isozaki, K., Tsujimura, T., Nomura, S., Morii, E., Koshimizu, U., Nishimune, Y., Kitamura, Y., 1994. Cell type-specific deficiency of c-kit gene expression in mutant mice of mi/mi genotype. Am. J. Pathol. 145, 827–836.

Krosl, G., He, G., Lefrancois, M., Charron, F., Romeo, P.H., Jolicoeur, P., Kirsch, I.R., Nemer, M., Hoang, T., 1998. Transcription factor SCL is required for c-kit expression and c-Kit function in hemopoietic cells. J. Exp. Med. 188, 439–450.

Kutukova, N.A., Nazarov, P.G., Kudryavtseva, G.V., Shishkin, V.I., 2016. Mast cells and aging. Adv. Gerontol. 29, 586–593.

Li, Z., Liu, S., Xu, J., Zhang, X., Han, D., Liu, J., Xia, M., Yi, L., Shen, Q., Xu, S., Lu, L., Cao, X., 2018. Adult connective tissue-resident mast cells originate from late erythro-myeloid progenitors. Immunity 49 (640–653), e645.

Liu, J., Divoux, A., Sun, J., Zhang, J., Clement, K., Glickman, J.N., Sukhova, G.K., Wolters, P.J., Du, J., Gorgun, C.Z., Doria, A., Libby, P., Blumberg, R.S., Kahn, B.B., Hotamisligil, G.S., Shi, G.P., 2009. Genetic deficiency and pharmacological stabilization of mast cells reduce diet-induced obesity and diabetes in mice. Nat. Med. 15, 940–945.

Loewendorf, A.I., Matynia, A., Saribekyan, H., Gross, N., Csete, M., Harrington, M., 2016. Roads less traveled: sexual dimorphism and mast cell contributions to migraine pathology. Front. Immunol. 7, 140.

Mackey, E., Ayyadurai, S., Pohl, C.S., S, D.C., Li, Y., Moeser, A.J., 2016. Sexual dimorphism in the mast cell transcriptome and the pathophysiological responses to immunological and psychological stress. Biol. Sex. Differ. 7, 60.

Pangas, S.A., 2012. Regulation of the ovarian reserve by members of the transforming growth factor beta family. Mol. Reprod. Dev. 79, 666–679.

Pellegrini, M., Filipponi, D., Gori, M., Barrios, F., Lolicato, F., Grimaldi, P., Rossi, P., Jannini, E.A., Geremia, R., Dolci, S., 2008. ATRA and KL promote differentiation toward the meiotic program of male germ cells. Cell Cycle 7, 3878–3888.

Rossi, V., Lispi, M., Longobardi, S., Mattei, M., Di Rella, F., Salustri, A., De Felici, M., Klinger, F.G., 2017. LH prevents cisplatin-induced apoptosis in oocytes and preserves female fertility in mouse. Cell Death Differ. 24, 72–82.

Todaro, F., Campolo, F., Barrios, F., Pellegrini, M., Di Cesare, S., Tessarollo, L., Rossi, P., Jannini, E.A., Dolci, S., 2019. Regulation of kit expression in early mouse embryos and ES cells. Stem Cells 37, 332–344.
Valent, P., Bettelheim, P., 1992. Cell surface structures on human basophils and mast cells: biochemical and functional characterization. Adv. Immunol. 52, 333–423.
Webb, L.M., Lieberman, P., 2006. Anaphylaxis: a review of 601 cases. Ann. Allergy Asthma Immunol. 97, 39–43.
Yamazaki, M., Tsujimura, T., Morii, E., Isozaki, K., Onoue, H., Nomura, S., Kitamura, Y., 1994. C-kit gene is expressed by skin mast cells in embryos but not in puppies of Wsh/Wsh mice: age-dependent abolishment of c-kit gene expression. Blood 83, 3509–3516.
Zierau, O., Zenclussen, A.C., Jensen, F., 2012. Role of female sex hormones, estradiol and progesterone, in mast cell behavior. Front. Immunol. 3, 169.